Northumbria
University
NEWCASTLE

Study of mechanical performance of polymer nanocomposites reinforced with exfoliated Graphite of different mesh sizes using Micro-indentation

S. Khammassi (a,*), M. Tarfaoui (a,*), K. Lafdi (b,c)

(a) ENSTA Bretagne, IRDL - UMR CNRS 6027, F-29200 Brest, France.

(b) University of Dayton, OH 45469, USA

(c) Northumbria University, Newcastle upon Tyne, NE1 8ST, United Kingdom

*Corresponding author. E-mail address: sabrine.khammassi@ensta-bretagne.org

*Corresponding author. E-mail address: mostapha.tarfaoui@ensta-bretagne.org

Abstract

The first phase of this work aims to use the right additive nano-fillers choices, such as exfoliated Graphite (ExG), increasing the mechanical, electrical, and thermal performances. In this work, we are interested in quantifying the effect particles' size on a polymer matrix's performance. For this, three sets of exfoliated polymers filled with Graphite, characterized by three particle sizes, called meshes 50, 100, and 150, were investigated. In this analysis, exfoliated Graphite reinforced polymers were subjected to indentation tests to define local mechanical properties. The sample is an epoxy 862 matrix reinforced with exfoliated graphite additives. For each specific size, the additives are mixed in percentages of 0 % in the act of control, 0.5 %, 4 %, 8 %, and 16 % by

weight. Matching pure polymers, polymers reinforced by exfoliated Graphite have proven to have significant improvements in local elastic properties (such as modulus, hardness, stiffness, etc.). Results showed that the reinforced epoxy's local mechanical properties are affected by the size and the percentage of nano-additives. Through the inspection of the load-displacement curve, it can be concluded that the nano-additive has a significant influence on the plastic mechanical properties of the sample. Therefore, the size of nanoparticles has significantly improved in material properties.

Keywords: Polymer matrix, nanofillers, Exfoliated Graphite, Indentation, Mechanical proprieties.

Introduction

Polymer materials as epoxy resins are widely used in various applications, such as transportation, building materials, electronics, sports goods, consumer goods, etc. [1] [2]. Therefore, composite materials are widely used in modern aircraft and marine structures due to their superior properties [3] [4] [5] [6]. The most logical reasons for their use are significant strength-to-weight ratio, high resistance of corrosion, fatigue resistance, and flexibility to be fabricated under challenging shapes [7] [8] [9]. Furthermore, using neat materials are certainly limited due to their inherent properties. In this case, new polymer materials with good performance reach considerable attention to improve polymer properties and enlarge their applications to new areas. Thus, they hold good strength to weight ratios and are easy to process, and have a low cost [10]. However, pure polymeric applications such as epoxy materials are generally confined due to their basic low thermal, electrical conductivity, and ductile mechanical properties.

According to the mechanical point mentioned earlier, pure epoxy resin has lower impact strength and lower elongation at break, making it brittle. However, its hardness and rigidity are sufficient for packaging and have various uses. For this suppose, several researchers aim at including reinforcements into this matrix. Their primary role is to increase the mechanical properties such as stiffness, tensile strength, hardness, fatigue, etc. However, they are also intended to improve physical properties such as fire characteristics or mechanical abrasion, temperature sensitivity, or electrical properties. To improve the monolithic epoxy mechanical characteristic, many scientists have applied nanoparticles like graphene, carbon black, carbon nanotubes, and more carbonaceous materials to emphasize it because of their significant elasticity modulus and capacity to avoid propagation of crack [3] [11] [12] [13] [14]. To be more precise, graphene has developed to be approved like reinforcement filler for various polymer matrices. Otherwise, polymers with nano-fillers have received much care in current years because they have highly sought after multifunctionality characteristics [15].

Among the fundamental approaches is adding nano-fillers to build nanocomposites [16]. Fillers are performed to reduce material costs and to improve their life period. Including nano-fillers into polymers create a significant increase in their properties (electrical, thermal, and mechanical) and, consequently, their multifunctionality [17]ï [21]. This enhancement of the composites performances [5] counts mostly on the filler source, filler type, preparation and treatment technique [2], the nano-fillers particles size and shape, definite surface area, surface growth the degree, the energy of the surface, and the mode of nanoparticles partition into a polymer matrix [16].

In this case, several carbon additives have been used to improve the neat polymer proprieties [22]. Carbon blacks, carbon nanotubes, and carbon nanofiber present the majority as it is

mentioned in numerous investigations [12] [23][12], [24], [25]. Most carbon nanocomposite reach enhances the neat polymers mechanical properties due to nanotubes' stiffness and strength [25] [26]. However, the unreasonably high nanotubes cost is the critical block to employ it in such an area. To reduce their huge prices [10] and the inappropriate handling associated with them [27], it is better to produce nanofillers. For example, exfoliated Graphite is mentioned in this case as replacement reinforcement into polymer improvement, which is a light carbon material with a couple of unique characteristics such as resistance to aggressive media, improved specific surface area, and flexibility [2] [12] [28]. The SEM image in Figure 1 presents the exfoliated graphite morphology.

Deleted: -

Deleted: ,

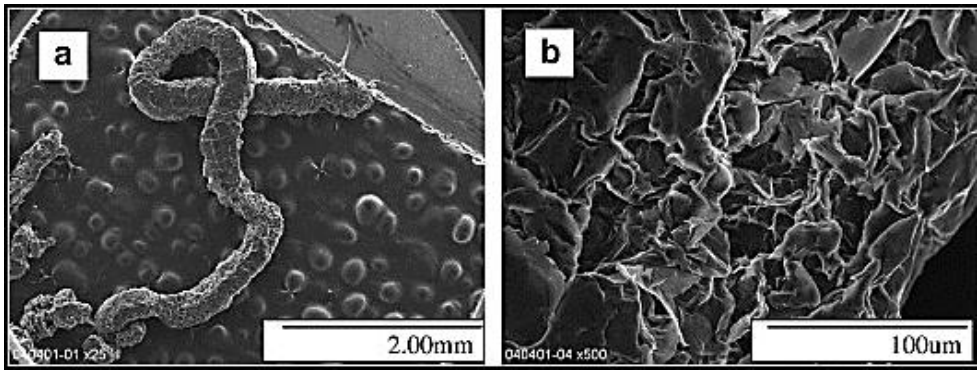

Figure 1: Exfoliated graphite morphology

Furthermore, it is discovered by many researchers that the additions of exfoliated Graphite limit the weight loss; this means an increase in the wear resistance. This is due to the vital surface area for ExG that improves the degree of interaction [2]. Therefore, the size of the ExG has to be prudently chosen to optimize the performance of polymers [28].

Wang et al. [29] revealed that an increase in epoxy toughness largely depends on the graphene sheets' size. Zhao and Hoa [30] studied the effect of two-dimensional nanofillers' particle size on

improving epoxy's toughness. They reported that the stress concentration factor decreases as the particle size decreases, and when the particle size is less than 1 ε m, the stress concentration factor does not change. Recently, Chatterjee et al. [10] reported that the larger the size of graphene nanosheets, the greater the enhancement of epoxy resin fracture toughness, which contradicts Zhao's simulation results. Other studies have shown that graphene's surface area is a critical parameter. As the surface area of ExGs increases the stress transfer from the polymer to the nanosheet. A recent theoretical study by Han et al. [31] predicted that the minimum density of 3D graphene components is inversely proportional to their building blocks' size. The large surface of ExG has good dispersion due to its strong van der Waals force and stacking between ´-´ planes [29]. All of these studies have caused enormous challenges and many questions remain unanswered such as the effect of graphene size on mechanical properties and resin cross-linking.

Deleted:

Deleted: ¶

Deleted: arudiws

Deleted: ¶

Deleted: s

In this study, an attempt was made to demonstrate the impact of size nano-additives on ExG/epoxy composites' local mechanical properties. We compared three ExGs with different surface areas (sheet sizes are 16.02 m^2/g, 15.61 m^2/g, and 15.35 m^2/g). Different amounts of ExG (0.5wt%, 4wt%, 8wt%, 12wt%, 16wt%) were used to synthesize composite materials, and their mechanical properties were studied. To understand the ExG size effect more accurately, a micro indentation test campaign was carried out in this work to describe the local mechanical properties as a function of the size of the graphene particles (MESH) and their different weight percentages. The results show a strong dependence on the properties of the materials (Young modulus, resistance, elastic and plastic energy) with the size and the percentage of the graphene particles.

Deleted: .

Materials

The samples are an epoxy matrix reinforced by the exfoliated graphite additives, which are divided into 3 groups, which are characterized by their size: (1) 50 MESH, (2) 100 MESH, and (3) 150 MESH. These additives were incorporated at levels of 0 wt.% as a control, 0.5 wt.%, 4 wt.%, 8 wt.%, and 16 wt.% in each group. Figure 2 gives a schematic representation of the 3 meshes of ExG into the epoxy matrix considered in this work.

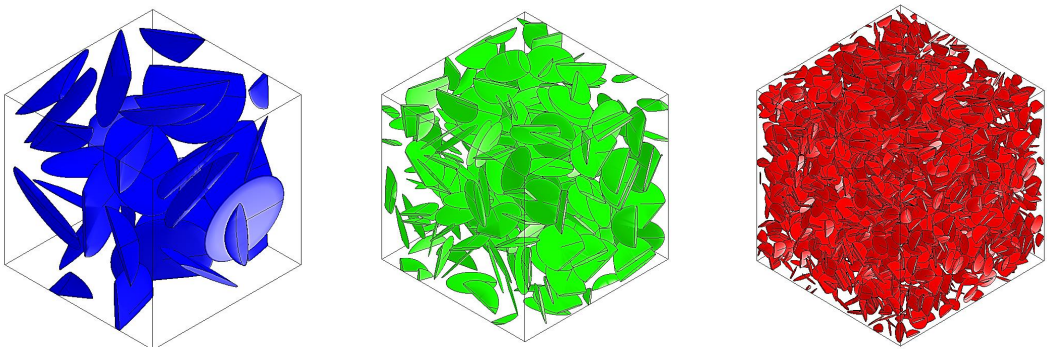

(a) 8wt.% (50 mesh) *(b) 8wt.% (100 mesh)* *(c) 8wt.% (150 mesh)*

Figure 2: Different way of ExG distribution with the three different meshes.

The epoxy used in these samples is EPON Resin 862. The Graphite employed for these tests was natural flake graphite with a diameter of 500 µm. Exfoliated Graphite was made as described below: a combination of nitric and sulfuric acid and natural Graphite was applied. After 24 h of reaction, intercalation with the graphene sheets appears to create an intercalated graphite compound. The next step was the mixture's filtration, then washed with water and dried using an oven at low temperatures. The intercalated graphite compound was exposed to a hasty heat treatment temperature of 900°C and a quick extension.

SEM carried out the morphological characterization of ExG nanofiller at three different magnifications: 1 mm, 100 µm, and 20 µm, Figure 3. SEM images of ExG nanofiller shows a cellular structure that is associated with a large expansion. The graphite before exfoliation is in the form of þakes, which have the graphite c-axis perpendicular to the plane of the þake. Because of the large expansion along the c-axis, the exfoliated þake becomes long in the direction that corresponds to the c-axis of the þake before exfoliation. Consequently, the ExG made from a graphite þake looks like a worm, as shown in the SEM image at low magnification (1 mm), Figure 3a, and high magniýcation (100 µm), Figure 3b. However, at 20um magnification, Figure 3c, we can observe graphene sheets with thickness ranging from 1 nm to about 16 nm and diameters ranging from sub-micrometer to hundreds of µm). The distance between graphitic stacks is about 5-10 nm, Figure 3.

Formatted: Space After: 0 pt

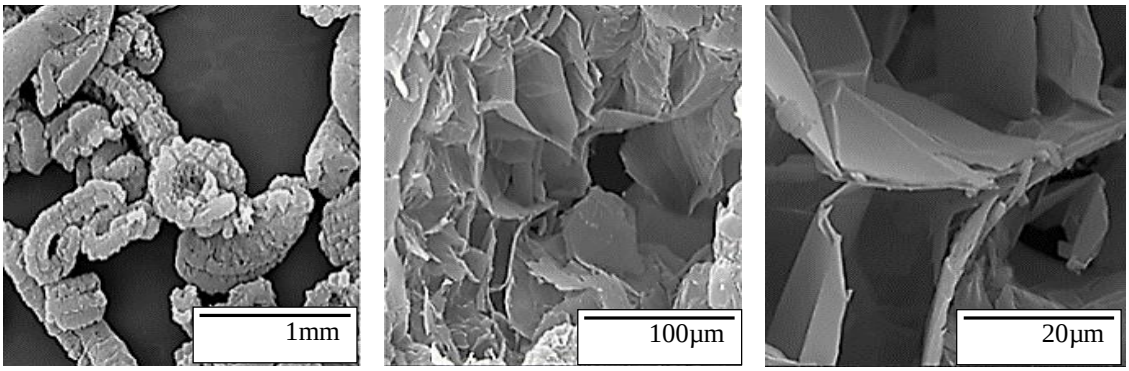

(a) *(b)* *(c)*

Figure 3: Exfoliated graphite morphological ExG nanofiller by SEM at three different magnifications (a) 1 mm, (b) 100 µm, (c) 20 µm

Formatted: Space After: 0 pt

The extension ratio was as high as 300 times. With the revision, three types of exfoliated Graphite filled polymers with different graphite particle dimensions were arranged. The graphite flakes were detached using 50, 100, and 150 mesh and are considered large, medium, and small flake polymers, Figure 4.

Deleted: it

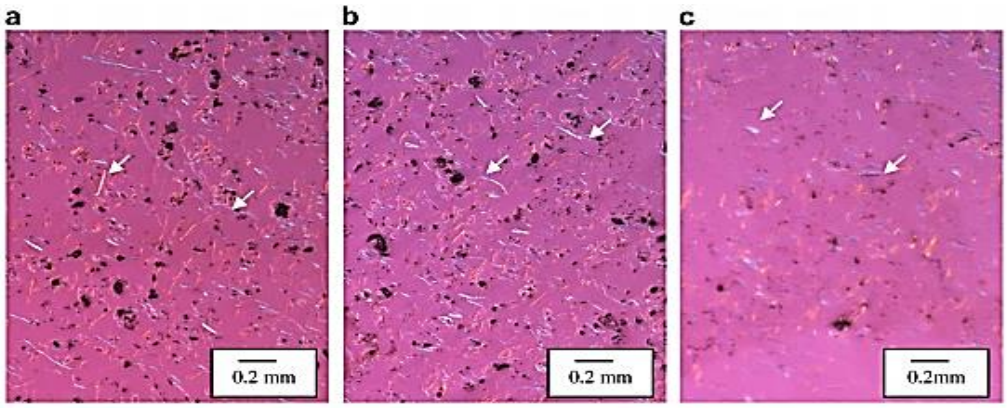

Figure 4: Light exfoliated Graphite filled polymers microscopy micrographs, (a) small (b) medium and (c) large flake, with the same graphite charging level (8 wt.%).

Materials holding the polymer concentration and exfoliated Graphite of 0.5 wt.%, 4 wt.%, 8 wt.%, 12 wt.%, and 16 wt.% were arranged. Initially, the exfoliated graphite flakes were significantly cropped by employing a homogenizer at a very significant rotation velocity (13500 turns/minute) in a solvent. The blade of the homogenizer rotates and cracks the larger graphite flakes to smaller nanosheets. Using ultrasonication further enhances the graphite nanosheets distribution. After the mixing procedure is accomplished, the mixture is crowd into a silicone rubber frame. The frame with the mixture was filled into a hydraulic press to cure. The curing conditions for the molds are hard-pressed under 10000 lb at 250 °F for 2 h and then at 350 °F for two more hours. To contribute to the distribution of the filler into the polymer, a resistivity scan was employed to estimate the resistivity value in the cured specimens; 64 data points were

obtained applying four-probe measurements. All specimens had displayed reliable resistivity values with a regular deviation of less than 4%.

Micro-indentation

Indentation test has been thoroughly applied to describe the local mechanical characteristic of diverse materials like composites [4] [5] [6][4], [25]. The micro-indentation test is one of the currently established methods to examine the composite materials interface properties, Figure 5. Using the indentation test, this study aims to quantify the effect of the size and the percentage of nanofillers on an epoxy resin's local mechanical behavior doped by ExG. Micro-indentation tests were released to define the local elastic mechanical properties. An example of representative indentation curves is given and studied for different weight fractions of ExG [12] [32].

The mechanical properties of reinforced epoxy with additives samples were estimated for each MESH for the levels of 0.5 wt.%, 4 wt.%, 8 wt.%, 12 wt.%, and 16 wt.%, by weight employing the indentation test. A CSM Micro-Hardness Tester with Vickers diamond indenter and a nominal angle of 136° was used. The micro-indentation parameters applied for the tests are: approach speed of 50000 nm/min, contact load of 20 mN, load rate of 2000 mN/min, unload rate of 2000 mN/min, maximum load of 1000 mN and 20 s of pause, Figure 6.

This micro-indentation test released in four steps:

- First step: Vickers indenter pecks the surface.
- Next step: Loading phase up until the maximum load (1000 mN).

- Third step: Holding the load. It was complete to keep away from the creep influence on the unloading characteristics.
- Final step: Unloading phase.

The article treats the results of tests associated with micromechanical characteristics: hardness, Young's modulus performed adopting the indentation technique. Because the samples' surface has a significant effect on the hardness rate, its examination before is very important. Consequently, micro-indentation procedures have to be severely regular, controlled with the necessities to be able to realized measurement on veritable narrow areas of the specimen [32].

A principal deduction would be that the micro-indentation experiment method is influential if it is correctly employed and if the results are correctly treated. Indeed, it has been presented that numerous parameters (polishing, decohesion determination, fiber splitting, fiber diameter, test facilities, etc.) have an essential effect on the absolute results. This presents some hesitation about the validity of the results if they are taken as absolute values. Nonetheless, if a set of diverse reinforced polymer specimens is verified under the same conditions, resulting in the same test and clarification procedures, the achieved interface properties' suitability has been verified [33].

Depending on these rectifications, Young's modulus is practically constant among all considered loads, as it is an intrinsic property. Although the load increase affects the decreases of hardness, which is generally assigned to the influence of the indentation size, it can be associated with the imprint's deformation.

The instrumented indentation test has been widely used and studied because of the ease with which it can be applied to estimate the materials mechanical properties from the force-displacement curve on small volumes of material. Elasticity and fracture toughness can also be

calculated from the force-displacement curves recorded. This technique allows studying the mechanical properties of materials at different scales [34].

Deleted: ¶
¶
¶
¶

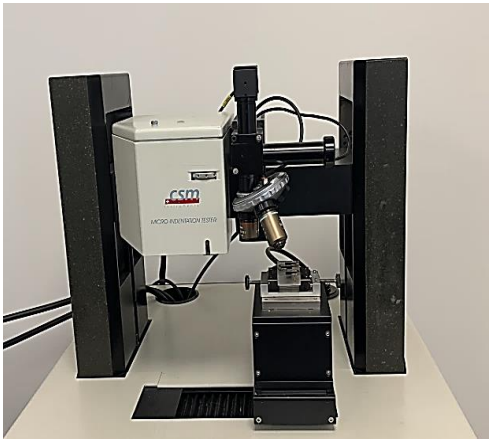

Figure 5: Image of the indentation machine and specimens under test.

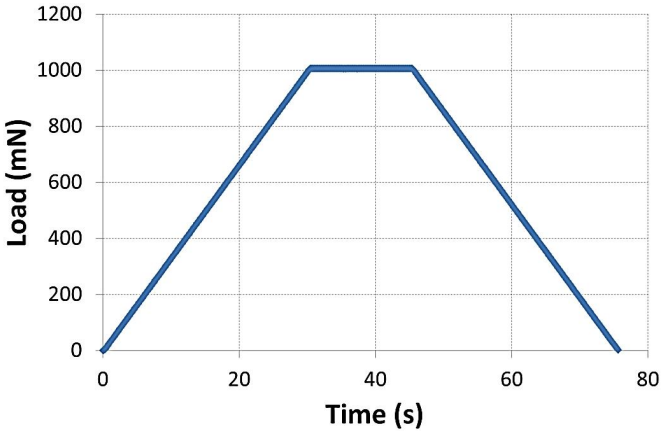

Figure 6: Load condition applied during the micro-indentation test.

The specific indication that we faced with the micro-indentation test is the indentation depths, which are, Figure 7:

h_t is the whole depth below a load P_t,

h_e is the elastic rebound depth for the unloading duration,

h_f is the depth of the residual impression,

h_a is the surface displacement at the perimeter,

h_p is the depth of the contact indentation.

Deleted: Depending on these rectifications, Young's modulus is practically constant among all considered loads, as it is an intrinsic property. Although the load increase affects the decreases of hardness, which is generally assigned to the influence of the indentation size, it can be associated with the imprint's deformation.

Deleted: The instrumented indentation test has been widely used and studied because of the ease with which it can be applied to estimate the materials mechanical properties from the force-displacement curve on small volumes of material. Elasticity and fracture toughness can also be calculated from the force-displacement curves recorded. This technique allows studying the mechanical properties of materials at different scales [34].¶

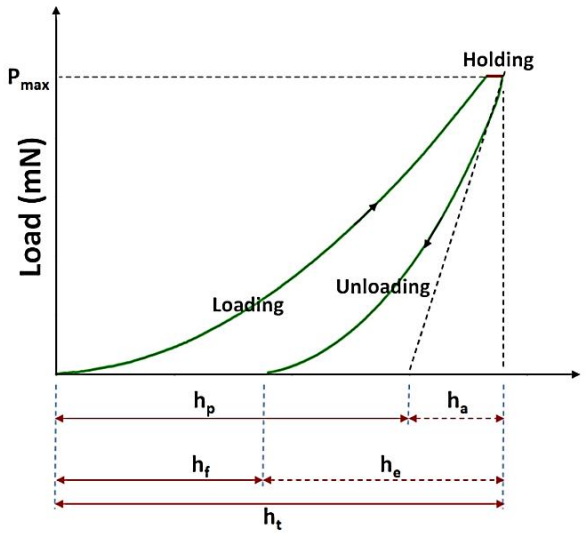

Figure 7: Indentation depths expression

Results

Load displacement behavior

Before presenting the different results of the micro indentation test, it is necessary to ensure the tests' reproducibility. Figure 8 shows that the tests present good reproducibility. The load-displacement curves for each reinforced epoxy exposed in Figure 9. These curves contribute to evaluate the elastic and plastic characteristics of the samples overall area. Figure 9 shows the Pï ŭ interactions of ExG/epoxy specimen computed with different percentage according to the different MESHS. Matched to the neat epoxy, the reinforced epoxy specimen shows an expressively significant indentation load (P) for some kind of nanofillers. Table 1 summarizes some important information from Figure 9 where the P-value at ŭ = 5 µm for 50, 100, and 150

MESH is increased respectively with adding nanoparticle compared to neat epoxy, which denotes that the reinforced nanofillers created an important involvement to the large indentation feedback of reinforced epoxy, Figure 9. Certainly, with the addition of the ExG nanoparticles, there is a stiffness increase, and, consequently, a displacement reduction for a force of 1000 mN, as it is in Figure 9. Matched to the neat epoxy, the displacement decreases by 11.51%, 12.62%, 13.43%, 20.026%, 24.52%, for 0.5wt.%, 4wt.%, 8wt.%, 12wt.% and 16wt.%, with 50 MESH. An increase of 7.84%, 11.42%, 12.67%, 17.37%, 20.42%, for 0.5wt.%, 4wt.%, 8wt.%, 12wt.% and 16wt.%, with 100 MESH, 7.31%, 10.42%, 12.01%, 15.52%, 16.65% for 0.5wt.%, 4wt.%, 8wt.%, 12wt.% and 16wt.%, with 150 MESH, as it is clear in Figure 10. These results proved that including ExGs into epoxy nanocomposite contributes to enhancing the toughness behavior by increasing the mass fraction at the different MESHS. This variation in mechanical behavior between the three types of materials (3 MESHES) is strongly linked to the size of the particles and the mode of distribution. Moreover, increasing the MESH size in each percentage will result in a more significant number of ExG particles, making more probability of getting more agglomeration.

For both neat epoxy and ExG reinforced epoxy nanocomposite specimen, the deformation under indentation test could not be improved after unloading, that denotes that their deformations were not elastic; there is dissimilarity concerning the curves of loading and unloading. Figures 8 and 9 show that as a type of the size of ExG change, the material changes' rigidity also.

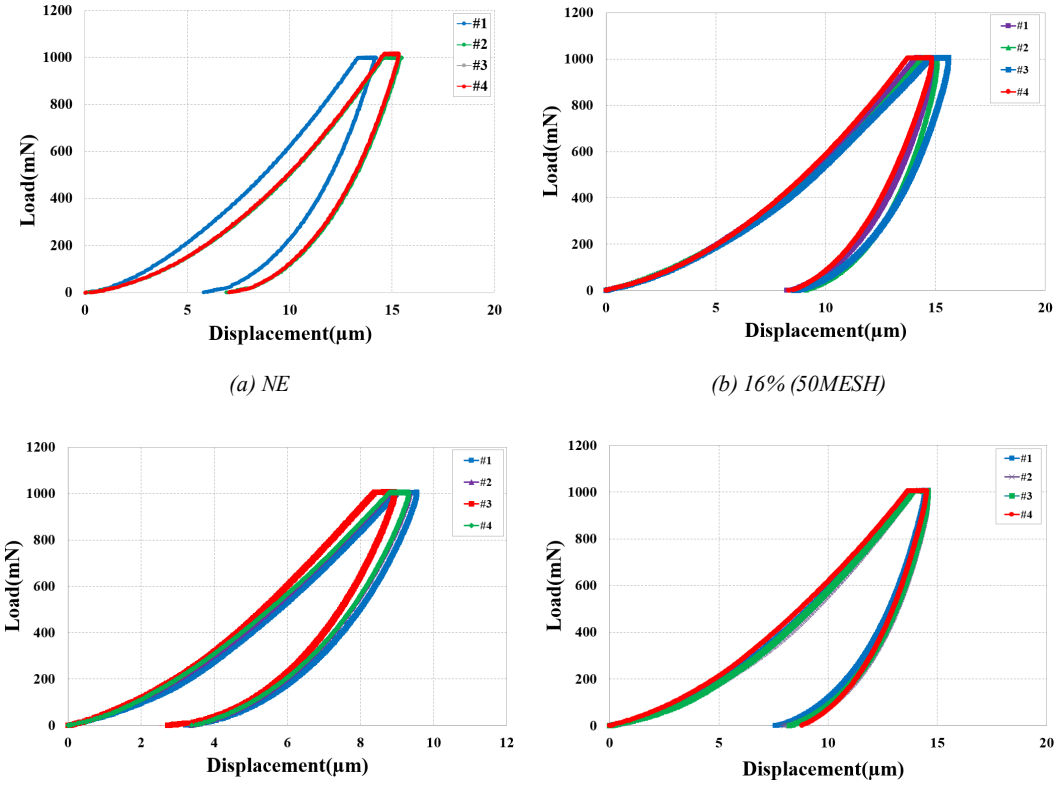

(a) NE

(b) 16% (50MESH)

(c) 16% (100MESH)

(d) 16% (150MESH)

Figure 8: Reproducibility of tests with NE and 16wt.% ExG with different mesh.

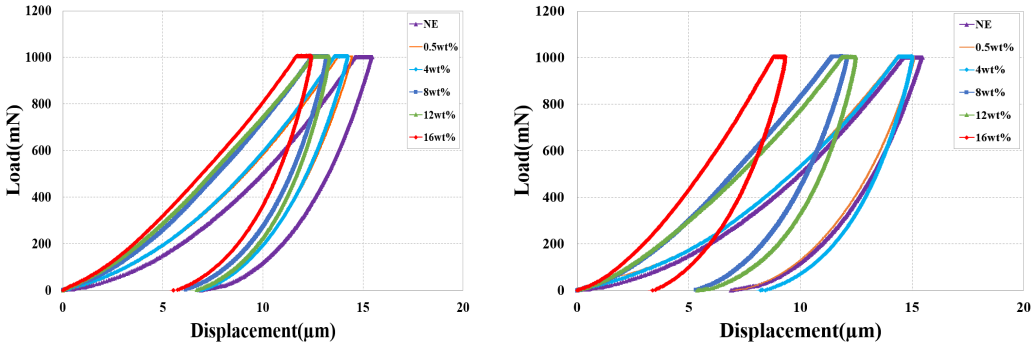

(a) 50 MESH

(b) 100 MESH

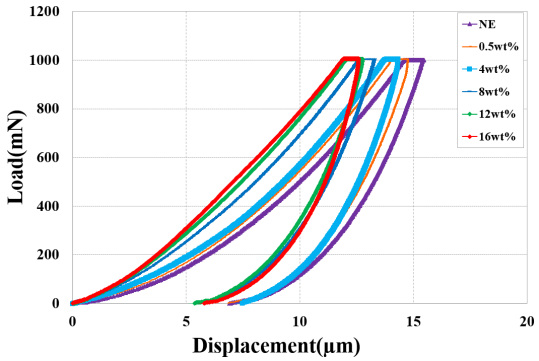

(c) 150 MESH

Figure 9: Pï ŭ interactions of ExG/epoxy specimen computed with different percentage according to the different mesh

Deleted:

Deleted: ¶

Table 1: Maximum indentation load (P) at ŭ = 5 µm

		Exfoliated Graphite (wt.%)					
% ExG	**Load**	**0**	**0.5**	**4**	**8**	**12**	**16**
50 MESH	Average	172,3399	250.751775	203.6071	187.3118	181.705333	208.566533
	St.D	34,4189114	65.6973137	25.0420697	38.3842567	61.9352659	57.2528076
100 MESH	Average	172,3399	193.178033	211.0679	253.208425	205.961033	341.678833
	St.D	34,4189114	41.612256	63.6900139	39.7876217	49.1368244	134.89312
150 MESH	Average	172,3399	202.318025	219.311967	212.663167	206.128067	215.94975
	St.D	34,4189114	38.5700221	77.5183532	35.5600152	40.7311457	48.728964

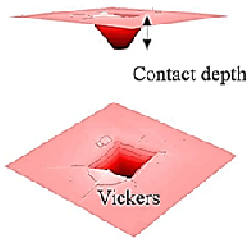

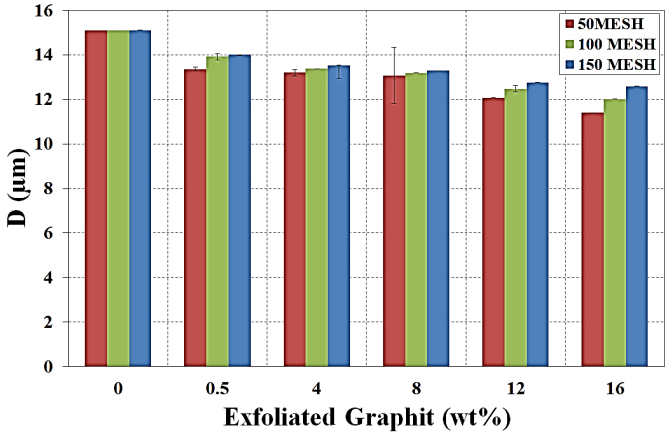

Figure 10: Effect of additives on the displacement of the reinforced epoxy

Young's modulus E

Figure 11 attaches the calculated Young's modulus as a function of nanofillers. Including 0.5 wt.%, 4 wt.%, 8 wt.%, 12 wt.%, and 16 wt.% in the epoxy matrix presents to have improved distribution particles and the structure resistance, thereby increasing the elastic modulus from 2.72 GPa to 12.08 GPa with 50 MESH, from 2.72 GPa to 9.40 GPa with 100 MESH and from 2.72 GPa to 8.09 GPa with 150 MESH. This enhancement is due to the significant aspect ratio and intrinsic ExG mechanical performance compared to the neat epoxy.

Adequate and uniformly distributed nanosheets can increase epoxy strength and increase its load-bearing capacity by increasing the mass fraction of ExG. In this case, it seems that there is good interaction between the fillers and the polymer matrix. There is an evident interfacial bond between the fillers and the matrix where it proves the vital role of including graphene into epoxy. The stress transfer from the matrix to the filler particles and the particles helps to transfer this stress from particle to particle until reaching the entire structure, thereby increasing the nanocomposite's strength. The significant modules are seen with the bigger size, corresponding to the 50 MESH, Figure 11. The large surface area of graphene at 50MESH creates a severe interaction with the epoxy matrix than the smaller size. The larger surface area of ExGs increases the contact area with the epoxy826 matrix, thereby maximizing the stress transfer from the epoxy826 to the graphene nanosheets, which explain in turn the important youngs modulus with 50 MESH.

Deleted:

Accordingly, this vital influence of the size of the ExGs can be explained by the existence of rigid graphite sheets that contribute in their turn to increase the modulus of the polymer. Besides, it seems that the higher degrees of alignment could be possible because of the lower density of

the large size of ExGs epoxy nanocomposite sheets, compared to small and medium sheets size. In this case, the large size with a high aspect ratio has a lower concentration, where it has highly aligned sheets and a high orientation factor composed of high-quality and low-defect graphene sheets, which favors the better elastic modulus.

Moreover, the platy shape of exfoliated Graphite, which increases aspect ratio and increases surface area contributes to obtaining a sheet that cannot be easily cracked with a small extent of bending or tensile force. These results suggest that a significant ExG dimension will limit and absorb the shock effect and transfer that save the matrix against failure [27] [35].

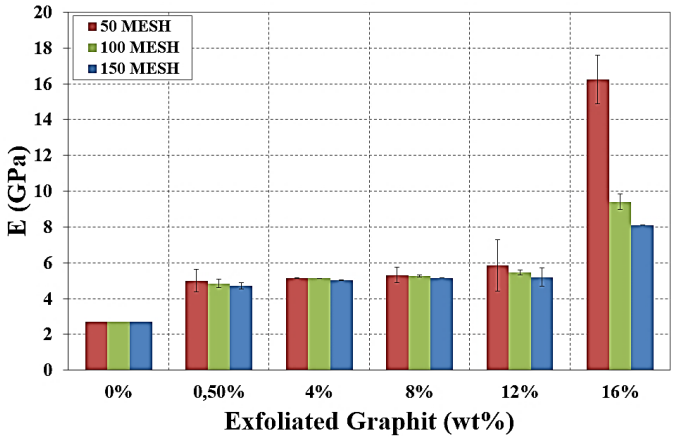

Figure 11: Effect of additives on Young modulus

Hardness Hv

Figure 12 shows the effect of a different kind of nanofillers content on the ExG reinforced epoxy nanocomposite's hardness. An important enhancement in hardness was detected with the addition of ExG nano-particles. The neat epoxy specimen show a hardness of 26.56 (Kgf/mm^2)

VICKERS, which enlarges to 46.247 (+74.12%), 48.03 (+80.83%), 53.225 (+100.39%) and 57.769 (+117.50%) for the 50 MESH size. An increase to 41 (+54.36%), 46.43 (+74.81%), 44.7 (+68.29%), 45.88 (+72.74%), 55.486 (+108.9%) for the 100 MESH, and an increase to 41.554 (+56.45%), 44.14 (+66.18%), 43.402 (+63.41%), 44.685 (+68.24%), 51.831 (+95.14%) for the 150 MESH, with the addition of 0.5wt.%, 4wt.%, 8wt.%, 12wt.% and 16wt.% by weight ExG, respectively. This increase in hardness Hv with the increase of ExG mass fractions is due to respectable distribution and interfacial bonding amongst nanofillers and the epoxy matrix. The hardness Hv increase is observed with the different MESH sizes but different degrees. The most significant enhancement is presented with the smaller MESH (50 MESH), which coincides with the larger size of ExG. Besides, the high surface area of exfoliated graphene has proven that when the graphene filler is uniformly dispersed in the epoxy matrix, the nanocomposite's performance has the potential to be maximized. Therefore, compared with the smaller size, the large size of ExGs seems to produce such a uniform dispersion, which helps increase the reinforced structure's toughness. Except that the large surface of ExG has good dispersion due to its strong van der Waals force and the ´ -´ inter-planer stacking, the important hardness Hv of ExG reinforced epoxy nanocomposite enhanced with large size (small mesh).

Deleted:

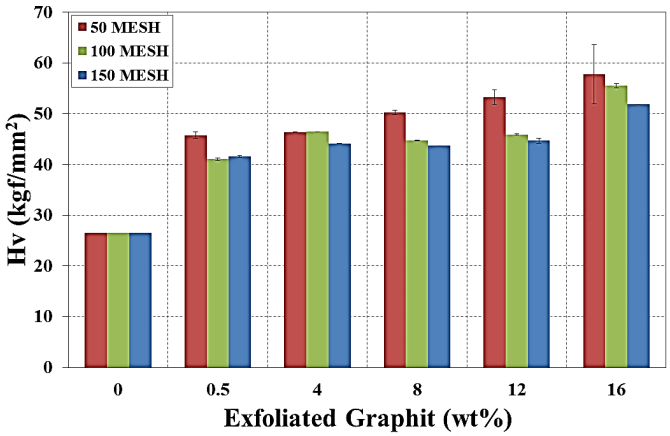

Figure 12: Effect of additives type on reinforced epoxy hardness.

Stiffness S

Figure 13 demonstrates that the reinforced epoxy matrix with 0.5 wt.%, 4 wt.%, 8 wt.%, 12 wt.%, and 16 wt.% of ExG has better resistance indentation compared to the discrete neat epoxy. Thus, it seems that the biggest size of ExG, 50 MESH, shows the most important improvement among the three meshes for all percentages. Therefore, particle size nano-fillers' effect on improving epoxy's toughness has an essential impact on reinforcing epoxy nanocomposites. These results prove that as the particle size decreases, the stiffness factor decreases. In this case, large size with a high aspect ratio has a lower stress concentration, in which there are highly aligned flakes and a high orientation factor composed of high-quality and low-defect graphene flakes, resulting in significant stiffness of nanocomposite structure.

Deleted: a

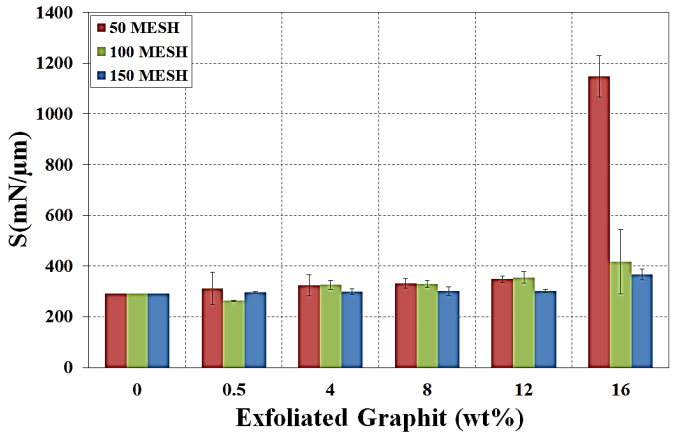

Figure 13: Effect of additives type on stiffness Energies

Formatted: Centered

Deleted: ¶

As shown in Figure 14, during the micro indentation procedure, elastic-plastic deformation occurred. During unloading, plastic energy is stored, and elastic energy is recovered. The difference in elastic and plastic energies showed that each material had different mechanical properties. Calculate the elastic W_{elas} and plastic W_{plas} energy according to the equation (1) (2) (3).

$$W_{tot} = \int_0^{h_t} P dh \quad (1)$$

$$W_{elas} - \int_{h_f}^{h_t} P dh \ (2) \quad (2)$$

$$W_{plas} = W_{tot} - W_{elas} \ (3) \quad (3)$$

In the equations, W_{tot}, W_{elas}, W_{plas}, P, h, h_f, and h_t are the total energy, elastic energy, plastic energy, load of the indenter, depth of penetration, residual depth, and maximum depth.

Figure 15(a) and Figure 15(b) shows the calculated value of elastic energy and plastic energy in the micro-indentation test. Generally, plastic energy increases with increasing nanofillers concentration. The plastic energy as a quantitative reflection of the viscosity effect is due to the internal friction inside the polymer/composite [36] [37]. The plastic properties of ExG/Epoxy826 nanocomposites continue to increase until the ExG concentration reaches 16 wt%. Besides, as shown in Figure 15(b), an abnormal reduction phenomenon was observed for the 16 wt% ExG/Epoxy826 nanocomposite, which was attributed to the apparent agglomeration of EXG in the nanocomposite. Adding a high percentage of ExGs, tend to cluster and create the agglomeration leading to the degradation evolution of the mechanical properties. Including high mass, fraction gives the ability to the graphene sheets to be loosely connected and agglomerated. The agglomeration of nanoparticles reduces the potential enhancement of nanocomposites' mechanical properties due to the interfacial area restriction and can be simply destroyed by mechanical force. Besides large, medium, small surface area, However, agglomeration of graphene nanoparticles at high mass fraction could result in different levels that depend on the nanofiller's distribution manner.

Deleted: ,

In addition, toughness is related to the energy absorbed, where higher toughness means that higher energy can be absorbed in the plastic area before breaking. In this work, based on the 12% weight of the composite material, the bigger size 50 MESH EXG showed the best results. The medium-sized 100 MESH exfoliated graphite shows second-best results than 150 MESH. The higher the toughness, the higher the material's ability to ensure design safety due to no small amount of plastic properties where it can be verified in Figure 16 using the Keyence microscope. Based on Figure 15, one can see the brittleness or ductility evidence of different materials (pure epoxy resin 826 and reinforced epoxy resin 828 nanocomposite). Referring to Figure 15, neat

epoxy 826 does not show relevant plastic areas and is therefore considered brittle (they have lower toughness values). According to the graph in Figure 15 (b), the transition threshold between brittleness and ductility behavior can be set to the maximum value of plasticity of 50 MESH. If the material's toughness is lower than this value, it can be considered brittle; otherwise, it exhibits important plastic behavior.

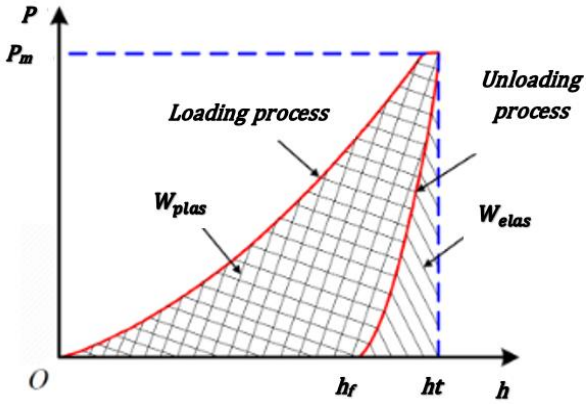

Figure 14: Schematic diagram of plastic properties and elastic properties in micro-indentation

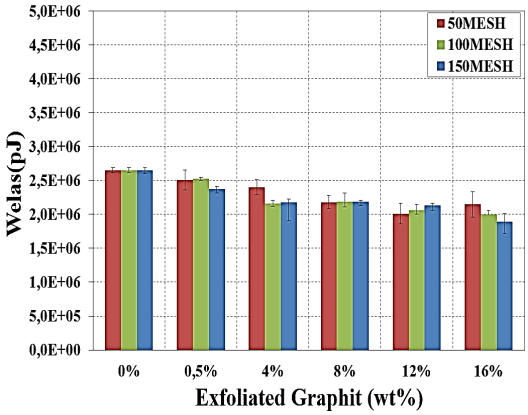

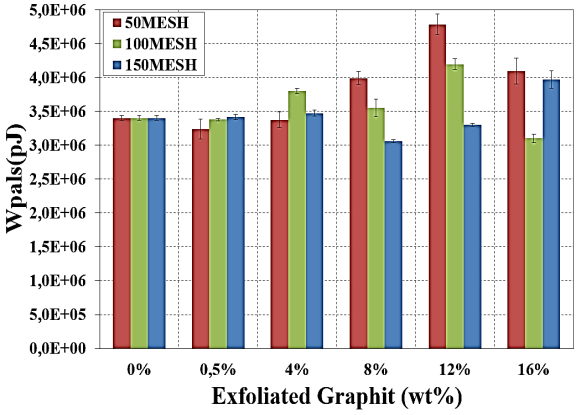

Figure 15: Effect of different mass fraction of EXG on the W_{elas} and W_{plas} with various MESH

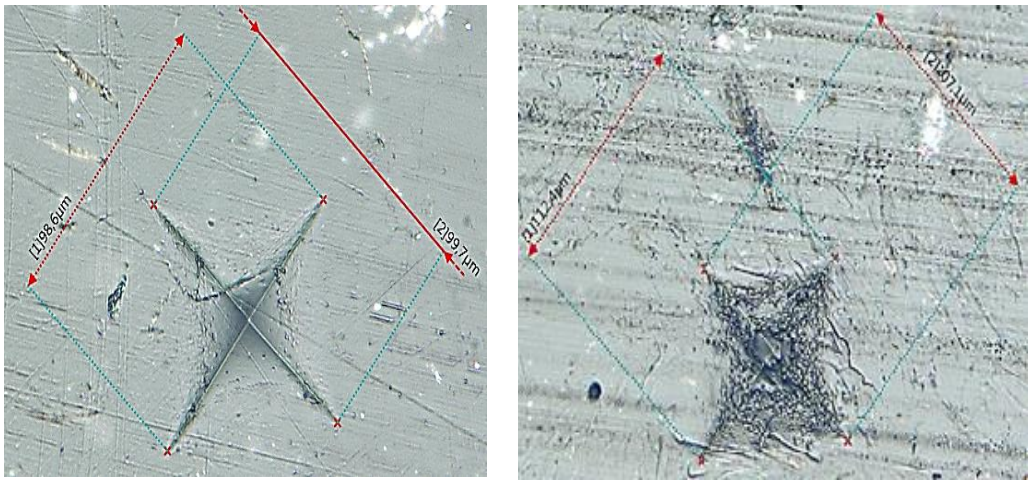

0.5wt.% for 50 MESH *16wt.% for 50MESH*

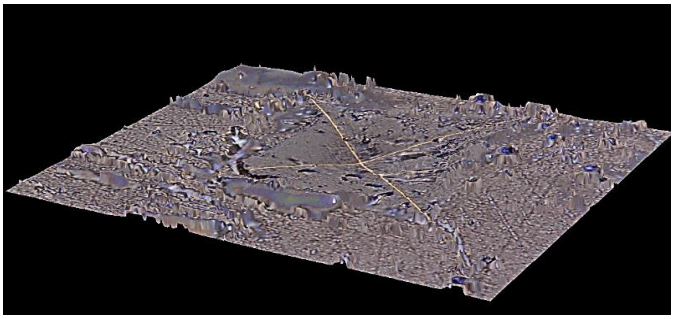

Figure 16: Residual indents obtained after instrumented micro-indentation using KEYENCE

Synthesis

Table 2 includes mechanical behavior and properties of all samples of exfoliated graphite/epoxy nanocomposites i.e. all percentages of exfoliated graphene with the three different sizes as 50, 100, 150 MESH.

Table 2 : Synthesis of the mechanical properties of the EXG/Epoxy nanocomposite with different size

wt.%	Mesh	**E (GPa)**	**D_{max} (µm)**	**Hv (Vickers)**	**S (mN/µm)**	**W_{elas} (pJ)**	**W_{plas} (pJ)**
0		4,3847	15	42,14	262,28	2,6E+06	3,4E+06
0.5	***50***	4,9953	14,365	45,75	312,14	2,5E+06	3,2E+06
	100	4,8460	13,92	41,01	263,19	2,5E+06	3,4E+06
	150	4,7218	14	41,55	296,49	2,4E+06	3,4E+06
4	***50***	5,1428	14,106	46,36	323,88	2,4E+06	3,4E+06
	100	5,1266	13,38	46,43	325,66	2,1E+06	3,8E+06
	150	5,0299	13,53	44,14	298,57	2,3E+06	3,9E+06
8	***50***	5,3156	14,075	50,23	331,55	2,2E+06	4,0E+06
	100	5,2617	13,19	44,70	328,95	2,1E+06	3,8E+06
	150	5,1538	13,29	43,70	300,44	2,4E+06	3,6E+06
12	***50***	5,8562	13,31	53,23	348,68	2,0E+06	4,8E+06
	100	5,4426	12,48	45,89	355,23	2,0E+06	4,2E+06
	150	5,1925	12,76	44,69	300,96	2,3E+06	3,5E+06
16	***50***	16,2403	12,4	57,77	1147,91	2,0E+06	4,2E+06
	100	9,4046	12,02	55,49	417,08	1,9E+06	2,5E+06
	150	8,096	12,59	51,83	367,22	1,9E+06	4,0E+06

Conclusion

Local mechanical properties of a reinforced epoxy matrix with different percentages of nanofillers as 0.5 wt.%, 4 wt.%, 8 wt.%, 12 wt.%, and 16 wt.% ExG additives were examined using depth-sensing micro-indentation, and this it depends on three groups 50, 100, 150 MESH. Adding a low percentage weight of ExG for all the kinds of mesh was studied as an important approach to enhance the epoxy matrix mechanical properties. The different percentages were dispersed in the epoxy matrix, creating a reinforced polymer. This work concentrated on the influence of the nanofillers additional nature on mechanical performance. It was established that including the bigger size 50 MESH to epoxy matrix reduces the indentation depth (ŭ) and raises the Young modulus (E), Stiffness (S), and hardness (H) as useful compared with other MESH. The micro-indentation tool has arranged a new method to estimate the extent and local mechanical properties of nano-dispersion additives in the micrometer range. The local mechanical properties provide typical overall performance. This work presents that the indentation test could be a useful technique in describing the reinforced polymer mechanical properties with nano-additives. It shows that the epoxy specimen's local mechanical properties were enhanced, such as a nano-additives change to better as the amount of nano-additive increases according to the bigger MESH size. Depending on the curve displacement and surface imaging, the influence of nano-additives on the entire plastic's mechanical properties is evident, and the size of ExG nano-additives has a significant practical effect on enhancing the characteristics of epoxy resins.

Deleted: ¶
¶
¶

References

[1] G. Chen *et al.*, ñPreparation and characterization of graphite nanosheets from ultrasonic powdering technique,ò *Carbon N. Y.*, vol. 42, no. 4, pp. 753ï 759, 2004, doi: https://doi.org/10.1016/j.carbon.2003.12.074.

[2] A. Mousa, ñThe effect of exfoliated graphite on the thermal properties of dynamically vulcanized PS/SBR composites,ò 2014.

[3] T. Mostapha, ñExperimental investigation of dynamic compression and damage kinetics of glass/epoxy laminated composites under high strain rate compression,ò *Adv. Compos. Mater. Anal.*, pp. 359ï 380, 2011.

[4] O. R. Shah and M. Tarfaoui, ñDetermination of mode I & II strain energy release rates in composite foam core sandwiches. An experimental study of the composite foam core interfacial fracture resistance,ò *Compos. Part B Eng.*, vol. 111, pp. 134ï 142, 2017, doi: https://doi.org/10.1016/j.compositesb.2016.11.044.

[5] M. Tarfaoui, M. Nachtane, H. Khadimallah, and D. Saifaoui, ñSimulation of mechanical behavior and damage of a large composite wind turbine blade under critical loads,ò *Appl. Compos. Mater.*, vol. 25, no. 2, pp. 237ï 254, 2018.

[6] M. Nachtane, M. Tarfaoui, D. Saifaoui, A. El Moumen, O. H. Hassoon, and H. Benyahia, ñEvaluation of durability of composite materials applied to renewable marine energy: Case of ducted tidal turbine,ò *Energy Reports*, vol. 4, pp. 31ï 40, 2018.

[7] M. Tarfaoui, S. Choukri, and A. Nême, ñEffect of fibre orientation on mechanical properties of the laminated polymer composites subjected to out-of-plane high strain rate compressive loadings,ò *Compos. Sci. Technol.*, vol. 68, no. 2, pp. 477ï 485, 2008.

[8] O. H. Hassoon, M. Tarfaoui, A. E. M. Alaoui, and A. El Moumen, ñExperimental and numerical investigation on the dynamic response of sandwich composite panels under hydrodynamic slamming loads,ò *Compos. Struct.*, vol. 178, pp. 297ï 307, 2017.

[9] O. H. Hassoon, M. Tarfaoui, A. E. M. Alaoui, and A. El Moumen, ñMechanical behavior of composite structures subjected to constant slamming impact velocity: An experimental and numerical investigation,ò *Int. J. Mech. Sci.*, vol. 144, pp. 618ï 627, 2018.

[10] S. Chatterjee, F. Nafezarefi, N. H. Tai, L. Schlagenhauf, F. A. Nüesch, and B. T. T. Chu, ñSize and synergy effects of nanofiller hybrids including graphene nanoplatelets and carbon nanotubes in mechanical properties of epoxy

composites,ò *Carbon N. Y.*, vol. 50, no. 15, pp. 5380ï 5386, 2012.

[11] M. Tarfaoui, ñStatic and dynamic behavior of nano filled polymer based composites,ò 2017.

[12] M. Tarfaoui, K. Lafdi, I. Beloufa, D. Daloia, and A. Muhsan, ñEffect of graphene nano-additives on the local mechanical behavior of derived polymer nanocomposites,ò *Polymers (Basel).*, vol. 10, no. 6, p. 667, 2018.

[13] A. El Moumen, M. Tarfaoui, M. Nachtane, and K. Lafdi, ñCarbon nanotubes as a player to improve mechanical shock wave absorption,ò *Compos. Part B Eng.*, vol. 164, pp. 67ï 71, 2019.

[14] M. Tarfaoui, A. El Moumen, and K. Lafdi, ñProgressive damage modeling in carbon fibers/carbon nanotubes reinforced polymer composites,ò *Compos. Part B Eng.*, vol. 112, pp. 185ï 195, 2017.

[15] M. Tarfaoui, K. Lafdi, and A. El Moumen, ñPerformance of polymer composites reinforced with carbon nanotubes,ò 2017.

[16] D. Cho, S. Lee, G. Yang, H. Fukushima, and L. T. Drzal, ñDynamic Mechanical and Thermal Properties of Phenylethynyl ‐ Terminated Polyimide Composites Reinforced With Expanded Graphite Nanoplatelets,ò *Macromol. Mater. Eng.*, vol. 290, no. 3, pp. 179ï 187, 2005.

[17] manel chihi and M. T. and Y. Q. and C. B. and H. B. E. N. YAHYA, ñEffect of Carbon Nanotubes on the In-plane Dynamic Behavior of a Carbon/Epoxy Composite under high strain rate compression using SPHB,ò *Smart Mater. Struct.*, 2020, [Online]. Available: http://iopscience.iop.org/10.1088/1361-665X/ab83cd.

[18] Y. Qureshi, M. Tarfaoui, K. K. Lafdi, and K. Lafdi, ñReal-time strain monitoring and damage detection of composites in different directions of the applied load using a microscale flexible Nylon/Ag strain sensor,ò *Struct. Heal. Monit.*, vol. 19, no. 3, pp. 885ï 901, 2020.

[19] Y. Qureshi, M. Tarfaoui, K. K. Lafdi, and K. Lafdi, ñNanotechnology and development of strain sensor for damage detection,ò in *Advances in Structural Health Monitoring*, IntechOpen, 2019.

[20] Y. Qureshi, M. Tarfaoui, and K. Lafdi, ñMulti-mode real-time strain monitoring in composites using low vacuum carbon fibers as a strain sensor under different loading conditions,ò *Smart Mater. Struct.*, 2020.

[21] Y. Qureshi, M. Tarfaoui, K. K. Lafdi, and K. Lafdi, ñIn-Situ Monitoring, Identification and Quantification of Strain Deformation in Composites Under Cyclic Flexural Loading Using Nylon/Ag Fiber Sensor,ò *IEEE Sens. J.*, vol. 20, no. 10, pp. 5492ï 5500, 2020.

[22] A. El Moumen, M. Tarfaoui, and K. Lafdi, ñMultifunctional composites based carbon nanotubes for marine energy conversion systems,ò 2017.

[23] M. K. Hassanzadeh-Aghdam, M. J. Mahmoodi, and R. Ansari, ñCreep performance of CNT polymer nanocomposites-An emphasis on viscoelastic interphase and CNT agglomeration,ò *Compos. Part B Eng.*, vol. 168, pp. 274ï 281, 2019.

[24] M. Tarfaoui, K. Lafdi, and A. El Moumen, ñMechanical properties of carbon nanotubes based polymer composites,ò *Compos. Part B Eng.*, vol. 103, pp. 113ï 121, 2016.

[25] B. Debelak and K. Lafdi, ñUse of exfoliated graphite filler to enhance polymer physical properties,ò *Carbon N. Y.*, vol. 45, no. 9, pp. 1727ï 1734, 2007.

[26] A. El Moumen, M. Tarfaoui, and K. Lafdi, ñMechanical characterization of carbon nanotubes based polymer composites using indentation tests,ò *Compos. Part B Eng.*, vol. 114, pp. 1ï 7, 2017.

[27] A. El Moumen, M. Tarfaoui, K. Lafdi, and H. Benyahia, ñDynamic properties of carbon nanotubes reinforced carbon fibers/epoxy textile composites under low velocity impact,ò *Compos. Part B Eng.*, vol. 125, pp. 1ï 8, 2017.

[28] S. Khammassi and M. Tarfaoui, ñInfluence of exfoliated graphite filler size on the electrical, thermal, and mechanical polymer properties,ò *J. Compos. Mater.*, 2020, doi: 10.1177/0021998320918639.

[29] X. Wang, J. Jin, and M. Song, ñAn investigation of the mechanism of graphene toughening epoxy,ò *Carbon N. Y.*, vol. 65, pp. 324ï 333, 2013.

[30] Q. Zhao and S. V Hoa, ñToughening mechanism of epoxy resins with micro/nano particles,ò *J. Compos. Mater.*, vol. 41, no. 2, pp. 201ï 219, 2007.

[31] N. M. Han *et al.*, ñGraphene size-dependent multifunctional properties of unidirectional graphene aerogel/epoxy nanocomposites,ò *ACS Appl. Mater. Interfaces*, vol. 10, no. 7, pp. 6580ï 6592, 2018.

[32] Z. Kaszowska, M. Kot, D. Biağek-Kostecka, and A. Forczek-Sajdak, ñApplication of micro-indentation tests to assess the consolidation procedure of historic wall paintings,ò *J. Cult. Herit.*, vol. 36, pp. 286ï 296, 2019.

[33] M. Desaeger and I. Verpoest, ñOn the use of the micro-indentation test technique to measure the interfacial shear strength of fibre-reinforced polymer composites,ò *Compos. Sci. Technol.*, vol. 48, no. 1ï 4, pp. 215ï 226, 1993.

[34] S. Kossman, D. Chicot, and A. Iost, ñIndentation instrumentée multi-échelles

appliquée à lœétude des matériaux massifs métalliques,ò *Matériaux Tech.*, vol. 105, no. 1, p. 104, 2017.

[35] A. El Moumen, M. Tarfaoui, H. Benyahia, and K. Lafdi, ñMechanical behavior of carbon nanotubes-based polymer composites under impact tests,ò *J. Compos. Mater.*, vol. 53, no. 7, pp. 925ï 940, 2019.

[36] H. Nosrati, R. Sarraf-Mamoory, D. Q. S. Le, R. Z. Emameh, M. C. Perez, and C. E. Bünger, ñImproving the mechanical behavior of reduced graphene oxide/hydroxyapatite nanocomposites using gas injection into powders synthesis autoclave,ò *Sci. Rep.*, vol. 10, no. 1, pp. 1ï 13, 2020.

[37] P. Jagdale, A. A. Khan, M. Rovere, C. Rosso, and A. Taliaferro, ñMulti walled Carbon nano tubeï Strength to polymer composite,ò *Nanomater. Join.*, 2015.